Spacecraft–Spacecraft Radio-Metric Tracking: Signal Acquisition Requirements and Application to Mars Approach Navigation

R. D. Kahn
Tracking Systems and Applications Section

S. Thurman
Navigation Systems Section

C. Edwards
TDA Technology Development

Doppler and ranging measurements between spacecraft can be obtained only when the ratio of the total received signal power to noise power density (P_t/N_0) at the receiving spacecraft is sufficiently large that reliable signal detection can be achieved within a reasonable time period. In this article, the requirement on P_t/N_0 for reliable carrier signal detection is calculated as a function of various system parameters, including characteristics of the spacecraft computing hardware and a priori uncertainty in spacecraft–spacecraft relative velocity and acceleration. Also calculated is the P_t/N_0 requirement for reliable detection of a ranging signal, consisting of a carrier with pseudonoise (PN) phase modulation. Once the P_t/N_0 requirement is determined, then for a given set of assumed spacecraft telecommunication characteristics (transmitted signal power, antenna gains, and receiver noise temperatures) it is possible to calculate the maximum range at which a carrier signal or ranging signal may be acquired. For example, if a Mars lander and a spacecraft approaching Mars are each equipped with 1-m-diam antennas, the transmitted power is 5 W, and the receiver noise temperatures are 350 K, then S-band carrier signal acquisition can be achieved at ranges exceeding 10 million km. An error covariance analysis illustrates the utility of in situ Doppler and ranging measurements for Mars approach navigation. Covariance analysis results indicate that navigation accuracies of a few km can be achieved with either data type. The analysis also illustrates dependency of the achievable accuracy on the approach trajectory velocity.

I. Introduction

In recent years, there has been increased interest in pursuing an intensive program of lunar and Mars exploration. Conducting an expansive program of lunar and Mars exploration with multiple spacecraft will present new technical and operational challenges. For example, future missions to Mars may rely on aerobraking to achieve orbit insertion. The aerobraking technique reduces a spacecraft's propellent requirement, but imposes more stringent navigation constraints than have been needed for previous interplanetary missions. Simultaneous deployment of a large number of spacecraft at the Moon and/or Mars could place unprecedented demands on already taxed ground-based tracking resources. The need for greater navigational accuracy and the need to relieve the burden on ground-based antennas could both be addressed by making use of in situ radio-metric tracking measurements. Doppler and ranging measurements between spacecraft provide navigation information complementary to Earth-based techniques and could potentially decrease reliance on ground-based tracking.

This article investigates requirements for successful acquisition of in situ radio-metric data types and discusses potential measurement precision. An error covariance analysis has also been performed to investigate the navigation accuracy that can be achieved using Doppler and ranging measurements between a spacecraft approaching Mars and a Mars-orbiting satellite used as a navigation aid. The analysis was designed to build upon the results of similar studies conducted previously [1-4]. The error covariance analysis points out some of the most important trajectory and tracking system parameters that influence the navigation performance that can be obtained. While the mission scenario studied herein involves Mars, in situ radio tracking is also applicable to lunar spacecraft navigation, or to any other mission in which a radio beacon or another spacecraft is available near the target body and can be used as a navigation aid.

II. Carrier Signal Acquisition

To perform in situ Doppler measurements, one spacecraft tracks the phase of a carrier signal transmitted from a second spacecraft. If the measurement is one-way, the signal originates at the second spacecraft; in a two-way measurement, the signal is uplinked by the first spacecraft, coherently transponded by the second spacecraft, and then phase tracked by the first spacecraft. The Doppler shift on the received signal provides a direct measure of the relative line-of-sight velocity of the two spacecraft. While one-way measurements are more easily implemented, they are inferior to two-way measurements because an unknown frequency offset between the two spacecraft oscillators can cause a significant error in the inferred relative velocity of the spacecraft.

A. Detection Strategy

A simple signal detection strategy is depicted in Fig. 1. The incoming signal is mixed with a locally generated model; the resulting baseband signal is integrated for T sec; and N consecutive T-sec integrations are Fourier transformed. The resulting Fourier coefficients reflect signal or noise amplitude in N bins of width $1/(NT)$ Hz, centered at the model frequency (Fig. 2). In general, the a priori uncertainty of the signal frequency, $\Delta\nu$, will be larger than the frequency range, $1/T$ Hz, that can be searched with a single Fourier transform, so a number of different model frequencies will have to be tried before the signal is detected.

To determine whether the signal is present in a given frequency span (the range of frequencies probed by a single Fourier transform), an amplitude detection threshold is selected. It is desirable to have the threshold be sufficiently low so that the signal will almost always be detected when it is present, and sufficiently high so that noise will not often be mistaken for signal. If the amplitude in some Fourier resolution bin exceeds the threshold, then the same frequency model is used to process the next NT sec of data. If a signal is detected in the same bin in two consecutive Fourier transforms, then it is assumed that the true signal has been found, and phase-lock-loop tracking commences.

Note that in any given Fourier transform, it is possible that the noise amplitude in at least one Fourier resolution bin will exceed the amplitude detection threshold. If one requires 99-percent confidence of detecting the true signal twice consecutively when it is present, and 1-percent probability of mistaking noise for signal, one obtains a relation between N and $(P_t/N_0)T$ that is approximated by: $(P_t/N_0)T = 29N^{-0.92}$. The Appendix discusses how this equation is obtained.

If the signal is equally likely to lie anywhere within the search space, $\Delta\nu$, then the mean time to signal acquisition is $\overline{T}_{ACQ} \approx \Delta\nu NT^2/2$ [5]. The acquisition time is proportional to NT because that is the time required to accumulate data for each Fourier transform, and is proportional to $T\Delta\nu$ because the frequency search space contains $T\Delta\nu$ spans of width $(1/T)$ Hz.

Taken together, the equations $(P_t/N_0)T = 29N^{-0.92}$ and $\overline{T}_{ACQ} \approx \Delta\nu NT^2/2$ imply that for a given value of

either N, T, or NT, there is a functional relationship between $\overline{T}_{ACQ}/\Delta\nu$ and the minimum P_t/N_0 required for reliable signal acquisition (99-percent confidence of signal detection and 1-percent probability of false alarm). The contours in Fig. 3 illustrate these relationships. As an example, if $N = 1000$ and $T = 0.01$ sec, it is required that $(P_t/N_0) \geq 7$ dB-Hz. The corresponding value of $\overline{T}_{ACQ}/\Delta\nu$ is about 0.05 sec/Hz; e.g., for a frequency uncertainty of 1 kHz, the expected search duration is 50 sec.

It is important to realize that the quantities N and T are not free parameters. Constraints due to both spacecraft dynamics and hardware (and perhaps software) impose restrictions on the allowable values of N, T, and their product, NT.

1. Constraints on the Selection of N and T. Hardware on board the spacecraft dictates a maximum value of N and a minimum value for T. At present, Fourier transform chips that can operate on hundreds of points are commonplace. If N is constrained by hardware to be at most 1024, then the data dump interval, T, is greater than 10^{-4} sec over most of the range of P_t/N_0 in Fig. 3. A dump rate, $1/T$, of 10,000 Hz is well within the capabilities of existing ground-based hardware and may be feasible for space-qualified systems by the late 1990's.

2. Constraints on Data Collection Interval, NT. Constraints on the product NT result from unmodelled beacon accelerations and from oscillator drift, both of which cause the frequency, f, of the received signal to change in time. Signal detection can be severely impeded if the signal moves through many Fourier resolution bins over the time, NT, during which the data for a single Fourier transform are acquired. If it is required that the change in frequency due to an unmodelled acceleration, δa, over time NT be smaller than $1/(2NT)$ Hz (half the size of one Fourier resolution bin), then the following relation results:

$$NT \leq \sqrt{\frac{c}{2f\delta a}} \tag{1}$$

A change in frequency due to oscillator instability has an effect similar to an unmodelled acceleration. Let $\sigma_{y_i}(NT)$ be the Allan standard deviation of spacecraft i's oscillator. Then imposing a constraint analogous to the unmodelled acceleration constraint above yields

$$NT < \frac{1}{2f\sqrt{\sigma_{y_1}^2(NT) + \sigma_{y_2}^2(NT)}} \tag{2}$$

Contours corresponding to $NT = 10^n$ for $n = -2$ to 2 are plotted in Fig. 3.

3. Range of Frequencies to be Searched, $\Delta\nu$. The range of frequencies to be searched, $\Delta\nu$, is a function of the uncertainty in spacecraft–spacecraft relative velocity. Also, for one-way transmission (and for the uplink of a two-way measurement), $\Delta\nu$ depends on an unknown frequency offset in the transmitting spacecraft's reference oscillator.

If the spacecraft–spacecraft velocity uncertainty is δv, the corresponding uncertainty in carrier frequency is $\Delta\nu = f(\delta v/c)$. The day-to-day drift in carrier frequency due to oscillator instability depends on the quality of the spacecraft oscillator. If the oscillator is not temperature-stabilized, a 2.3-GHz (S-band) carrier frequency may vary by thousands of Hz. A highly stable oscillator has day-to-day variations much smaller than 1 Hz at S-band.

4. Example: Calculation of P_t/N_0 Requirement for Carrier Acquisition. The above information may be combined in order to calculate the P_t/N_0 requirement for reliable carrier acquisition.

As an example, suppose one spacecraft is fixed on the surface of Mars, while a second spacecraft is on approach to Mars. The spacecraft are equipped to transmit and receive a 2.3-GHz signal. It is desired that a carrier signal be acquired within 5 min. Neither spacecraft has a priori knowledge of the spacecraft–spacecraft relative velocity and acceleration.

Since the spacecraft have no a priori knowledge of their relative velocity, the range of frequencies to be searched, $\Delta\nu$, is the full spacecraft–spacecraft relative velocity. A typical Mars approach velocity is 4 km/sec, corresponding to a frequency search range of approximately 31 kHz at S-band. Since 5-min acquisition is desired, it is required that $\overline{T}_{ACQ}/\Delta\nu \lesssim 0.01$ sec/Hz.

The relative acceleration of the lander and approach spacecraft is principally due to Mars rotation, which imparts up to 0.017 m/sec^2 of acceleration to the lander. This unmodelled acceleration imposes the constraint $NT \leq 2$ sec. Equation (2) indicates that the upper bound on NT arising from oscillator stability is also 2 sec if the 2-sec Allan standard deviation of the spacecraft oscillators is smaller than 8×10^{-11} sec/sec.

The parameter constraints are summarized in Table 1. The constraints $\overline{T}_{ACQ}/\Delta\nu \lesssim 0.01$ sec/Hz and $NT \leq 2$ sec are represented by the unshaded region in Fig. 4. The minimum P_t/N_0 satisfying both constraints is approximately 13 dB-Hz.

Once the P_t/N_0 requirement is known, then if the spacecraft telecommunication characteristics are specified, one can determine the maximum range at which the carrier can be acquired. Figure 5 illustrates P_t/N_0 as a function of range between the Mars lander and approach spacecraft, for several different assumptions about the spacecraft telecommunications system. The tapering of the curves at smaller ranges is due to the increasing contribution of Mars to the system noise temperature.

III. Doppler Measurement Precision

Once a carrier signal has been detected, tracking the signal's phase is straightforward. Phase tracking precision depends on a variety of factors, including P_t/N_0 and oscillator stability. However, if the carrier can be tracked at all, then the point-to-point phase precision is much smaller than one RF cycle (e.g., 13 cm at S-band). Phase tracking precision does not significantly affect the accuracy with which the Mars approach spacecraft's state can be determined by fitting to an arc of beacon-spacecraft Doppler data. Determination of the approach spacecraft's state should be limited by other effects, such as unmodelled spacecraft accelerations.

IV. Ranging Signal Acquisition

A. Signal Structure

The ranging measurement is performed as follows: A spacecraft transmits a signal to a second spacecraft that locks onto the signal and coherently transponds it back to the first spacecraft. Two-way ranging offers the tremendous advantage of eliminating the problem of unknown spacecraft clock offsets that can significantly degrade the accuracy of a one-way measurement. However, the accuracy of the two-way measurement is still affected by the first spacecraft's clock instability over the round-trip light time. For example, if the spacecraft oscillator has an Allan variance of 10^{-11} sec/sec over time scales of minutes and the two-way light time is 100 sec (30 million km), then clock instability introduces a 30-cm error.

The ranging signal is assumed to be of the following form:

$$s(t) = A\cos(\omega_0 t + \beta PN(p, f_c, t - t_n) + \phi_0)$$

where

A = the signal amplitude

ω_0 = the carrier frequency

β = the modulation index, $0 < \beta < \pi/2$

PN = a pseudonoise sequence with period p and chip rate f_c

p = the period of the PN sequence

f_c = the chip rate of the PN sequence, i.e., $1/f_c$ is the chip duration, τ_c

t_n = the epoch of the PN sequence

ϕ_0 = the phase of the carrier signal at $t = 0$

Pseudonoise (PN) sequences [6] are a special class of sequences of 1's and -1's that can be generated by linear feedback shift registers. Individual elements of such a sequence will be referred to as "symbols." PN sequences are periodic; a given sequence consists of repetitions of a symbol pattern of length p symbols. For every integer n, there exists at least one PN sequence of period $2^n - 1$. If $r(j)$ is a PN sequence with period p, then the autocorrelation of $r(j)$, $R_p(i) = (1/p)\int_1^p r(j)r(j+1)dj$ is equal to 1 for $i =$ any integer multiple of p and is equal to $-1/p$ for all other i (Fig. 6). The chip rate, f_c, of a PN sequence is the rate at which symbol transitions occur.

During a two-way ranging measurement, the spacecraft originating the PN signal simultaneously receives a PN code that had been transmitted one round-trip light time earlier. The incoming PN code is offset from the current state of the uplink code by an amount equal to the round-trip light time divided by the chip duration, τ_c. This code offset can be determined by cross-correlating the received signal with the locally generated sequence. To ensure that such a two-way ranging measurement is unambiguous, it is required that the period of the PN sequence, $p\tau_c$, be larger than the a priori uncertainty in the spacecraft–spacecraft range. The relationship between the chip rate, PN period, and range ambiguity is plotted in Fig. 7. The ranging precision is proportional to the product of the chip duration and the precision with which the PN sequences can be aligned. If chip alignment precision of 1 percent can be achieved in the tracking loop, then a chip rate of 1 MHz corresponds to a ranging measurement precision of 3 m.

B. Ranging Signal Detection

The incoming signal is

$$s(t) = A\cos(\omega_0 t + \beta PN(p, f_c, t - t_n) + \phi_0)$$

and the locally generated model for the carrier is

$$\tilde{s}(t) = \exp\left[i(\tilde{\omega}_0 t + \beta PN(p, \tilde{f}_c, t - \tilde{t}_n))\right]$$

If the carrier is fully suppressed ($\beta = \pi/2$), then multiplication of the signal and model, followed by low-pass filtering, yields the following:

$$C(t) \equiv s(t)\,(\tilde{s}(t)) = \frac{A}{2} \exp\left[i\left((\tilde{\omega}_0 - \omega_0)t - \phi_0\right)\right]$$

$$\times \left[PN(p, f_c, t - t_n) PN(p, \tilde{f}_c, t - \tilde{t}_n)\right]$$

To detect the signal, it is necessary that the model parameters, $\tilde{\omega}_0, \tilde{f}_c$, and $\tilde{t}_n$, be adequately close to the actual signal parameters, ω_0, f_c, and t_n. However, it is possible to design the spacecraft so that the PN clock and the transmitted carrier frequency are both referenced to the same frequency standard. In this case, a search must be conducted only for ω_0 and t_n; the code frequency, f_c, is a deterministic function of the carrier frequency, ω_0.

The product of actual and model signals is integrated over T-sec intervals, and a set of N consecutive integrations is Fourier transformed. It is important that the time period NT be long enough that the product $PN(p, f_c, t - t_n)\left[PN(p, \tilde{f}_c, t - \tilde{t}_n)\right]$ approximates the PN autocorrelation function. The signal can be detected via the Fourier transform only when (1) the model frequency lies within $1/2T$ Hz of the actual frequency and (2) the difference between the model PN epoch and the true PN epoch is a fraction of a chip.

Since a given Fourier transform probes a region of frequency space of width $1/T$ Hz, centered at the model frequency, a total of $T\Delta\nu$ Fourier transforms are required to search a frequency range of $\Delta\nu$ Hz. Note, however, that a T-sec average of $\{signal \times model\}$ suffers an amplitude loss equal to[1] sinc $(T(\tilde{\omega}_0 - \omega_0/2)$; if the signal and model differ by $1/2T$ Hz, the corresponding loss in amplitude is about 40 percent. It may be advantageous, therefore, to space the frequency models by an amount $1/k_f T (k_f > 1)$ to reduce the distance between the signal and the best model frequency. Reducing the spacing between frequency models increases the number of models needed to cover the search space.

[1] S. A. Stephens, "An Analysis of FFT Tone Acquisition," JPL Interoffice Memorandum 335.1-92-14 (internal document), Jet Propulsion Laboratory, Pasadena, California, May 14, 1992.

Even if the model frequency is perfect, a fully suppressed carrier cannot be detected unless the model PN epoch is also close to truth (within a fraction of a chip). If the model PN epoch is stepped in single-chip increments, then the best PN code alignment achieved may be off by as much as 1/2 chip, resulting in a factor of two amplitude loss (see Fig. 6). In order to decrease the potential loss of amplitude due to fractional PN-code misalignment, one may conduct the search using smaller step sizes, at the cost of requiring additional models to cover the entire search space. If the step size is $1/k_c$ chip, then up to $k_c \times p$ offsets may need to be tested before the signal is detected.

The signal search space is illustrated in Fig. 8 for the case $k_f = 1$. The search space consists of $N_f \times N_s$ cells, where N_f is the number of model frequencies and N_s is the number of trial symbol offsets. Each Fourier transform of $\{signal \times model\}$ probes a range of $(1/T)$ Hz, centered at the model frequency. One method of performing a systematic search is to step through all possible model symbol offsets for a given model frequency. If the signal is not detected, the model frequency is then shifted by $1/T$ Hz. Thus, at each model frequency, N_s N-point Fourier transforms are performed. Assuming the Fourier transforms can be computed in real time, $N_s \times (NT)$ sec are spent searching at each model frequency. Unfortunately, it is possible that this search algorithm would miss the signal entirely if the incoming signal's frequency is changing with time (due to unmodelled spacecraft-spacecraft relative acceleration and oscillator drift).

The problem of a signal with a moving frequency may be addressed by taking the following two steps: (1) set k_f equal to 2, i.e., space the model frequencies by $1/2T$ Hz; each Fourier transform of $\{signal \times model\}$ will still probe a region in frequency space of width $1/T$ Hz, but the region probed by adjacent frequency models will now overlap by 50 percent; and (2) require that the change in signal frequency over a time $N_s \times (NT)$ be smaller than $(1/2T)$ Hz. Given an upper bound on the spacecraft spacecraft relative acceleration and oscillator drift, this requirement places a constraint on the allowable values of the parameters N_s, N, and T (the impact of this and other constraints is discussed later). The number of Fourier transforms required to search the entire two-dimensional space with this strategy is $2T\Delta\nu N_s$.

The signal detection procedure is the same as the carrier detection method discussed earlier. Model signals are sequentially tested by mixing with the incoming signal and then Fourier transforming N points acquired over NT sec. If a Fourier frequency bin has amplitude exceeding the detection threshold, then the same model is tested again. If

a second detection occurs, it is assumed that the signal has been found and phase- and delay-lock-loop tracking is commenced. The mean time to signal acquisition is $\overline{T}_{ACQ} \approx NT^2\Delta\nu N_s$. The mean time to acquisition could be significantly reduced if the spacecraft hardware is capable of processing multiple model signals in parallel.

If the signal power is known, the amplitude threshold can be selected so that the probability of signal detection when a signal is present, P_{detect}, is high (e.g., 99 percent), while the probability of a false alarm, P_{false}, is low (e.g., 1 percent). For a given probability of detection and probability of false alarm, there is a functional relationship between the quantities $(P_t/N_0)T$ and N. For $P_{detect} = 0.99, P_{false} = 0.01$, and $k_c = 2$ (symbol search proceeding in half-chip steps), the relationship between N and $(P_t/N_0)T$ is well-approximated by the following equation (see Appendix):

$$\frac{P_t}{N_0}T = 43N^{-0.91}$$

The contours in Fig. 9 are derived by combining the equations $\overline{T}_{ACQ} = NT^2\Delta\nu N_s$ and $(P_t/N_0)T = 43N^{-0.91}$. As in the case of pure carrier detection, there are a number of constraints that restrict the allowable values of N, T, and NT.

1. Constraint on NT Arising From Unmodelled Spacecraft Acceleration. The requirement that the change in signal frequency over a time $N_s \times (NT)$ be smaller than $(1/2T)$ Hz is expressed as follows:

$$\frac{d(f_0)}{dt} < \frac{1/2T}{N_s NT} \Rightarrow NT^2 < \frac{c}{2f_0 N_s \delta a}$$

Here f_0 is the carrier frequency, c is the speed of light, and δa is the unmodelled spacecraft acceleration. As in the case of simple carrier detection, it is also required that the time NT be small enough so that unmodelled spacecraft accelerations do not smear the signal over multiple Fourier frequency bins. Together, these two constraints are given by

$$NT < \sqrt{\frac{c}{2f_0\delta a}}\left(MIN\left(1, \sqrt{\frac{N}{N_s}}\right)\right) \qquad (3)$$

2. Constraint on NT Arising From Unmodelled Spacecraft Velocity. It is required that the unmodelled spacecraft–spacecraft relative velocity be small enough so that the range does not change by more than 1/2 chip ($\tau_c/2$ sec) over the NT sec during which data are collected for a Fourier transform.

$$NT < \frac{c\tau_c}{2\,\delta v} \qquad (4)$$

where δv is the unmodelled spacecraft–spacecraft relative velocity.

3. Oscillator Stability Requirements. The constraints on oscillator stability are analogous to the constraints on NT arising from unmodelled spacecraft acceleration and velocity.

In analogy with the acceleration constraint, it is required that the signal change by less than $(1/2T)$ Hz over $N_s \times (NT)$ sec, and also that the carrier frequency not move through many Fourier frequency bins over the NT sec during which data are acquired for the Fourier transform (Δ *frequency* $< 1/(2NT)$ over NT sec). Letting $\sigma_{y_i}(\tau)$ denote the τ-sec Allan standard deviation of spacecraft i's oscillator,

$$\sqrt{\sigma^2_{y_1}(N_sNT) + \sigma^2_{y_2}(N_sNT)} < \frac{1}{2\,Tf_0}$$
$$\sqrt{\sigma^2_{y_1}(NT) + \sigma^2_{y_2}(NT)} < \frac{1}{2\,f_0 NT} \qquad (5)$$

In analogy with the velocity constraint, it is required that oscillator drift not introduce a delay of more than $\tau_c/2$ sec over the NT sec during which data are acquired for a Fourier transform. This constraint is looser than that imposed by the above equations for chip rates smaller than the carrier frequency (the usual case).

4. Example: Calculation of P_t/N_0 Required for Ranging Signal Acquisition. Suppose that ranging measurements are to be performed between a spacecraft approaching Mars and a beacon spacecraft on the planet's surface. The carrier frequency is S-band, and the chipping rate is 1 MHz. The length of the PN code is 2047 symbols, corresponding to a two-way range ambiguity of 600 km. The ambiguity can be resolved via spacecraft position determinations resulting from routine Earth-based Doppler tracking of the two spacecraft.

The spacecraft are provided with a crude estimate of their relative velocity: 0.5 km/sec, equivalent to 4000 Hz at S-band. The spacecraft–spacecraft relative acceleration is not modelled. Until the approach spacecraft is

within the sphere of influence of Mars ($\lesssim$1 million km), the total relative acceleration of the spacecraft and beacon is 0.017 m/sec^2 due to Mars rotation. Finally, it is assumed that the spacecraft hardware is capable of performing 1024-point Fourier transforms.

The parameter constraints corresponding to a signal acquisition time of 5 min are summarized in Table 2. All four constraints are satisfied in the unshaded region of Fig. 10 bounded by the contours $N = 1024$ and $\overline{T}_{ACQ}/2N_s\Delta\nu = 10^{-5}$ sec/Hz. The minimum P_t/N_0 satisfying the constraints is approximately 28 dB-Hz. Equation (5) may now be applied to determine the oscillator stability requirements:

$$\sigma_y(409 \text{ sec}) < 2 \times 10^{-6} \text{ sec/sec}$$

$$\sigma_y(0.1 \text{ sec}) < 2 \times 10^{-9} \text{ sec/sec}$$

These Allan variances are easily met by non-temperature-stabilized crystal oscillators.

Figure 5 indicates that if both the lander and approach spacecraft are equipped with 1-m-diam antennas and mediocre receivers ($T_{rec} = 350$ K), a 5-W S-band signal is sufficient to enable a 28-dB-Hz signal power-to-noise density ratio at spacecraft separations of millions of kilometers.

V. Ranging Measurement Precision

To within a factor of order unity, the precision with which PN codes can be aligned with a delay lock loop is $1/\sqrt{2P_t/N_0T_{dwell}}$, where T_{dwell} is the integration time. The resulting ranging measurement precision is

$$\epsilon_\rho \text{ (meters)} \approx \frac{c\tau_c}{\sqrt{2P_t/N_0T_{dwell}}}$$

The exact expression for the ranging measurement precision depends on details of the delay-lock-loop design. In practice, due to dispersion effects in the processing signal path, the best alignment precision that can be achieved is between 0.01 and 0.001 chips.

The utility of ranging is to eliminate the unknown bias inherent in carrier phase (Doppler) measurements. Once this bias has been determined, range changes can be precisely tracked by measuring the carrier phase. The phase of the carrier can be recovered with precision of a fraction of an RF wavelength, even when the transmitted signal has a modulation index of $\pi/2$ (fully suppressed carrier).

VI. Error Covariance Analysis for Mars Approach Navigation

In this section, the navigational utility of in situ radio tracking is illustrated through some examples drawn from a hypothetical future Mars mission, in which a spacecraft approaching Mars acquires Doppler and ranging measurements from a Mars-orbiting communications relay satellite. Error covariance computations for a sequential estimation scheme were performed using approximate models of the approach spacecraft and relay satellite trajectories, and the Doppler and ranging measurement errors. This analysis was not designed to be an exhaustive treatment of the approach navigation problem, but merely to illustrate some of the more significant aspects of the use of in situ Doppler and ranging measurements in this type of application. It should be remembered that although the particular application discussed below refers to Mars, in situ radio tracking is also applicable to missions to the Moon and other target bodies where radio beacons or additional spacecraft may be used as navigation aids.

The error analysis was performed using the model parameters summarized in Table 3. The approach spacecraft was assumed to move on a hyperbolic path with respect to Mars; except for the final hours prior to arrival at periapsis, this assumption leads to a trajectory that is essentially rectilinear and of constant velocity. To illustrate the effect of different approach velocities on navigation performance, two different values of asymptotic approach velocity were considered, representative of the minimum and maximum possible values for low-energy ballistic Earth-to-Mars transfer trajectories. The radius of closest approach chosen for this study (3417 km) yields a periapsis altitude of about 20 km, which is representative of trajectories leading to a direct entry and landing, or the initiation of an aerobraking maneuver for orbit insertion. The Mars-orbiting relay satellite was assumed to be in a circular orbit with a 12-hr period. The spacecraft acceleration-process noise level used in this analysis is intended to account for the small, nongravitational forces (e.g., solar radiation pressure mismodelling, gas leaks from valves, and pressurized tanks) that act on an interplanetary spacecraft.

The navigational utility of both one-way integrated Doppler measurements and two-way ranging measurements has been investigated. Integrated Doppler data are effectively a measurement of the accumulative change in the spacecraft-to-spacecraft range over the contact period. As shown by the parameters given in Table 3, integrated Doppler provides a highly precise measurement of range, but with a large constant bias. The frequency drift uncertainty assumed for the Doppler measurements is represen-

tative of oscillator stability on the order of 10^{-12} sec/sec. Two-way ranging measurements are much less precise than Doppler measurements, but provide an accurate measure of the spacecraft–spacecraft separation (Table 3). As described earlier, acquisition of a ranging signal requires a more extensive search than simple carrier signal acquisition. For fixed assumptions about the spacecraft onboard computing resources and the desired mean time to signal acquisition, the requirement on P_t/N_0 is higher to support ranging acquisition. As a result, the acquisition range for ranging data is considerably smaller than for Doppler data.

The results of the error covariance analysis are summarized in Figs. 11 and 12. These figures show the uncertainties in the approach spacecraft encounter coordinates as a function of time prior to arrival, expressed in an aiming plane (B-plane) coordinate system.[2] Figure 11 shows the semimajor axis of the aiming plane dispersion ellipse and the linearized time-of-flight uncertainty (position uncertainty in the S unit direction divided by τ_∞) for an approach velocity of 3 km/sec, while Fig. 12 shows the same two quantities for an approach velocity of 6 km/sec. (Mars Observer's approach velocity was about 2.4 km/sec; MESUR Pathfinder's approach velocity will be about 5.5 km/sec.) Note that, in practice, delay-lock-loop tracking of a PN-modulated carrier signal enables recovery of the carrier phase, thus enabling simultaneous acquisition of ranging and integrated Doppler measurements. However, Figs. 11 and 12 show the navigational uncertainties resulting from the use of either data type independently, in order to illustrate differences in the abilities of the two data types to determine various components of the approach trajectory.

Both Figs. 11 and 12 illustrate a clear difference between Doppler and ranging performance. Since ranging data provide a direct measurement of the spacecraft–spacecraft separation, the time of flight (which in this case is essentially the spacecraft range) can be very accurately determined immediately upon acquisition. In contrast, Doppler data can only measure this component of the flight path indirectly and need to be collected for up to several days before sufficient information is obtained. This occurs because Doppler data depend upon the relative acceleration of the approach spacecraft and the relay satellite (which is inversely dependent upon their relative range) to determine the time of flight. Additional experimentation found that the approach-spacecraft acceleration process noise was the principal factor limiting the integrated Doppler's ability to determine the time of flight.

Figure 12 shows that when the approach velocity is relatively high, the smaller acquisition distance associated with two-way ranging results in the aiming plane dispersion ellipse of the approach spacecraft remaining relatively large until about 15 hr prior to arrival. If a final maneuver is needed to correct the spacecraft's aim point, this implies that the maneuver may have to be performed very near the arrival point, with the ensuing risk that there may not be sufficient time remaining to redetermine the trajectory and correct any maneuver execution errors that might have occurred. Thus, if large approach velocities must be accommodated, early acquisition of Doppler followed by joint acquisition of Doppler and ranging data would be desirable.

VII. Summary

The P_t/N_0 required for acquisition of carrier or ranging signals between two spacecraft is a function of a number of parameters, including a priori uncertainty in the spacecraft–spacecraft relative state, and the capabilities of the spacecraft processing hardware and software (e.g., the maximum number of points that can be Fourier transformed in real time). Once these parameters are specified for a given set of assumptions about the spacecraft telecommunications systems, one may calculate the maximum range at which a signal can be acquired. As an example, it has been shown that S-band radio-metric measurements between a Mars lander and Mars approach spacecraft equipped with 1-m-diam antennas are feasible over distances of millions of kilometers. The analysis presented here can easily be applied to a wide variety of other mission scenarios.

To illustrate the utility of in situ radio-metric measurements between spacecraft, a covariance analysis was performed for the case of Doppler and ranging measurements between a Mars orbiter and a spacecraft on Mars approach. The results obtained are consistent with previous studies, and suggest that approach navigation accuracies of a few kilometers at Mars may be obtained with either in situ Doppler or ranging measurements.

In the near-term, in situ ranging and Doppler data between spacecraft would likely be relayed to Earth for navigation processing. Ultimately, onboard computing resources could be used to perform the navigation updates, enabling a near-real-time in situ navigation capability.

[2] The aiming plane, or B-plane, coordinate system is defined by three unit vectors, $\boldsymbol{S}$, $\boldsymbol{T}$, and $\boldsymbol{R}$. $\boldsymbol{S}$ is parallel to the incoming asymptote of the approach hyperbola; $\boldsymbol{T}$ is parallel to the Martian equatorial plane; and $\boldsymbol{R}$ completes an orthogonal triad with $\boldsymbol{S}$ and $\boldsymbol{T}$. The aim point for a planetary encounter is defined by the miss vector, $\boldsymbol{B}$, which lies in the $\boldsymbol{T}$–$\boldsymbol{R}$ plane, and specifies where the point of closest approach would be if the target planet had no mass and did not deflect the spacecraft's flight path.

References

[1] A. S. Konopliv and L. J. Wood, "High-Accuracy Mars Approach Navigation with Radio-Metric and Optical Data," paper AIAA-90-2907, presented at the AIAA/AAS Astrodynamics Conference, Portland, Oregon, August 20–22, 1990.

[2] S. W. Shepperd, D. P. Fuhry, and T. J. Brand, "Onboard Preaerocapture Navigation Performance at Mars," paper AAS 91-119, presented at the AAS/AIAA Spaceflight Mechanics Meeting, Houston, Texas, February 11–13, 1991.

[3] S. W. Thurman and J. A. Estefan, "Mars Approach Navigation Using Doppler and Range Measurements to Surface Beacons and Orbiting Spacecraft," paper AAS 91-118, presented at the AAS/AIAA Spaceflight Mechanics Meeting, Houston, Texas, February 11–13, 1991.

[4] S. W. Thurman and S. E. Matousek, "Trajectory and Navigation System Design for Robotic and Piloted Missions to Mars," *The Telecommunications and Data Acquisition Progress Report 42-107, vol. July–September 1991*, Jet Propulsion Laboratory, Pasadena, California, pp. 113–131, November 15, 1991.

[5] M. K. Simon, J. K. Omura, R. A. Scholtz, and B. K. Levitt, *Spread Spectrum Communications*, vol. III, Rockville, Maryland: Computer Science Press, 1989.

[6] R. Dixon, *Spread Spectrum Systems*, New York: John Wiley and Sons, 1984.

Table 1. Parameter constraints for 5-min carrier signal acquisition between a Mars lander and a spacecraft on Mars approach.

Constraint	Reason
$\overline{T}_{ACQ}/\Delta\nu \lesssim 10^{-2}$ sec/Hz	5-min acquisition, $\Delta\nu = 31$ kHz
$NT < 2$ sec	Eq. (1) (unmodelled acceleration)

Table 2. Parameter constraints for 5-min ranging signal acquisition between a Mars lander and a spacecraft on Mars approach.

Constraint	Reason
$\overline{T}_{ACQ}/2N_s\Delta\nu \lesssim 10^{-5}$ sec/Hz	5-min acquisition, $\Delta\nu = 4000$ Hz, and $N_s = 4094$
$N < 1024$	Capability of Fourier transform chip on spacecraft
$NT < 0.03\sqrt{N}$ sec	Eq. (3) (unmodelled acceleration)
$NT < 0.3$ sec	Eq. (4) (unmodelled velocity)

Table 3. Mars approach navigation error analysis parameters.

Trajectory parameter	Value
Asymptotic approach velocity, $v\infty$	3 or 6 km/sec
Radius of closest approach	3417 km
Inclination of approach trajectory to Martian equator	+15 deg
Mars relay satellite orbital period	2 hr
Mars relay satellite inclination	0 deg
Spacecraft acceleration process noise (approach spacecraft and relay satellite)	1.4×10^{-5} m/sec/$\sqrt{\text{hr}}$
A priori state uncertainty (1σ)	**Value**
Approach spacecraft epoch position	100 km
Approach spacecraft epoch velocity	1 m/sec
Relay satellite epoch position	3 km
Relay satellite epoch velocity	0.1 m/sec
Doppler measurement parameter	**Value**
Maximum acquisition range	2×10^6 km
Additive random measurement noise	4 mm (1σ)
Accumulative random measurement noise	0.58 m^2/hr
Frequency drift stability	0.3 mm/sec (1σ, a priori)
Carrier phase bias uncertainty	100 km (1σ, a priori)
Ranging measurement parameter	**Value**
Maximum acquisition range	8×10^5 km
Additive random measurement noise	5 m (1σ)
Range bias uncertainty	15 m (1σ)

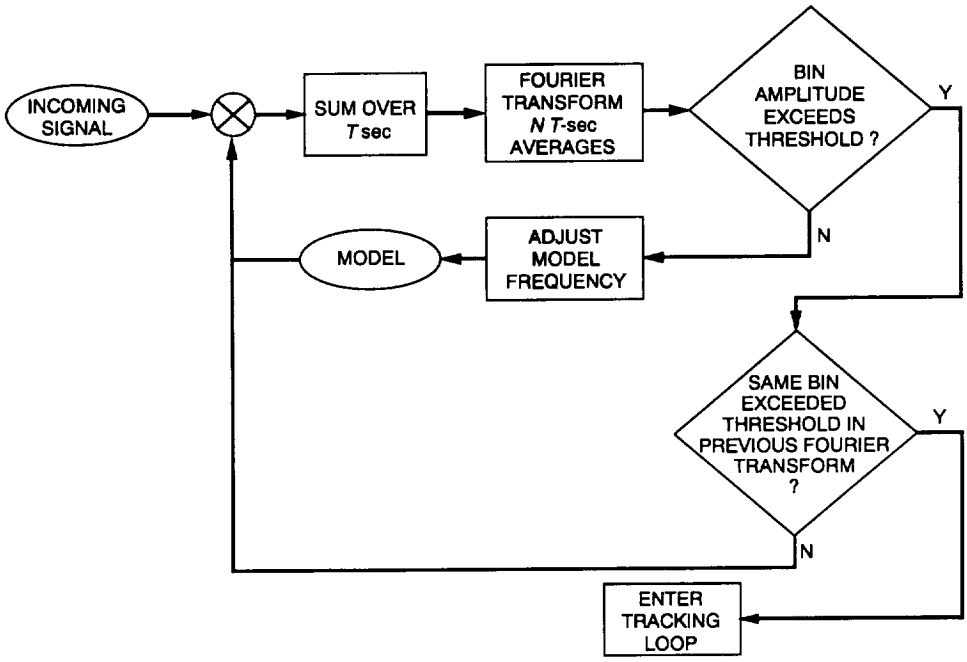

Fig. 1. A simple carrier signal detection strategy.

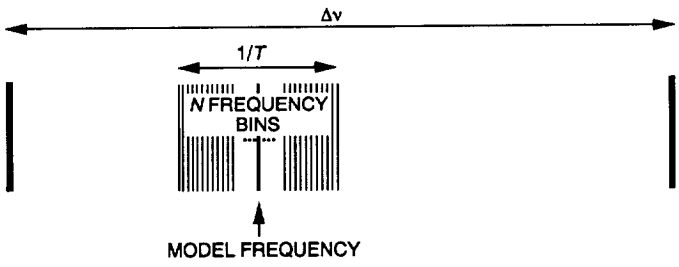

Fig. 2. The relationship between frequency search range, $\Delta\nu$ Hz, and frequency span, $1/T$ Hz, probed by a single Fourier transform.

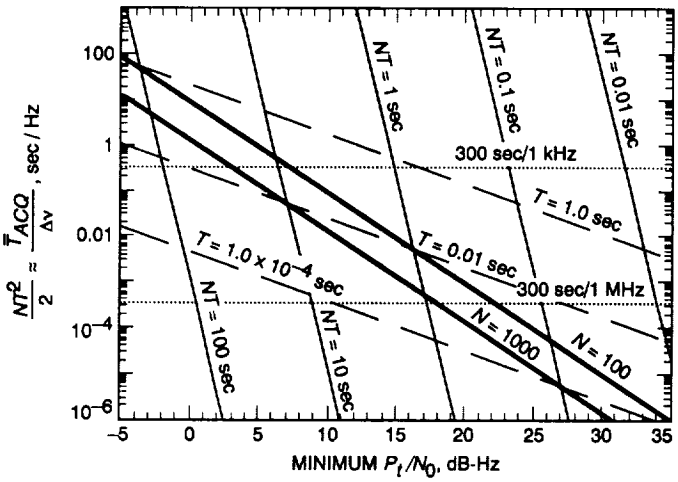

Fig. 3. Relationships between $T_{ACQ}/\Delta\nu$, N, T, and the minimum P_t/N_0 required for carrier signal acquisition with P_{false} = 0.01 while P_{detect} = 0.99.

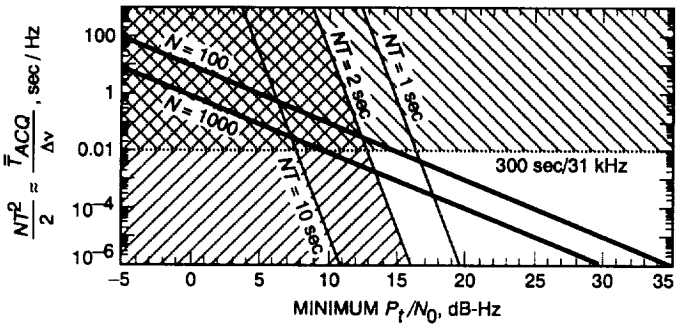

Fig. 4. Given the constraints $NT \leq 2$ sec and $T_{ACQ}/\Delta\nu \leq 0.01$ sec/Hz, the minimum P_t/N_0 needed for reliable carrier detection is 13 dB-Hz.

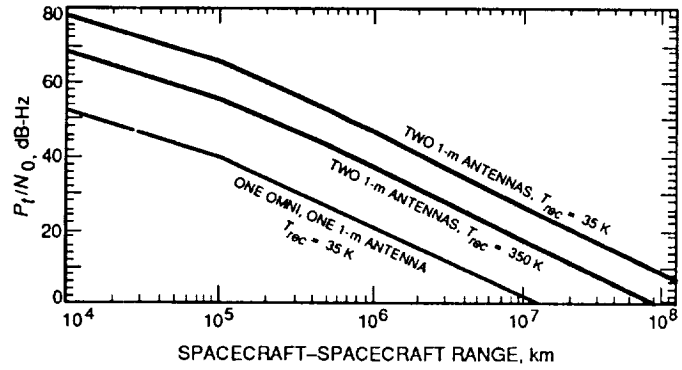

Fig. 5. P_t/N_0 as a function of Mars lander–approach spacecraft range. Transmitted power is 5 W. T_{rec} is the receiver noise temperature.

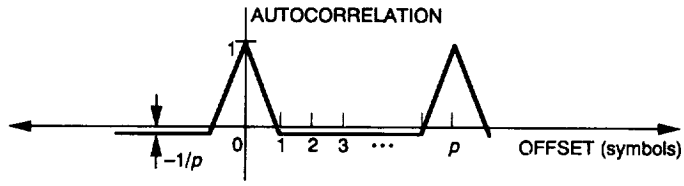

Fig. 6. Autocorrelation of a PN sequence of period p.

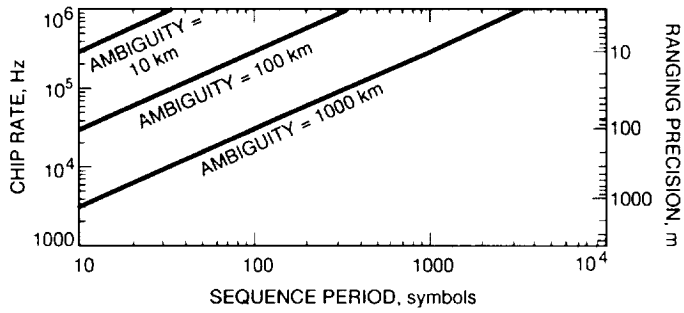

Fig. 7. Relationship between chip rate, length of PN sequence, range ambiguity, and ranging measurement precision (assumed tracking error is 1 percent of chip length).

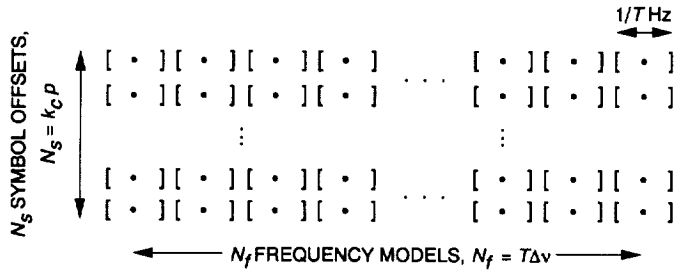

Fig. 8. Search space for carrier signal with PN phase modulation. Each bracket pair represents the range of frequencies probed by a Fourier transform of N T-sec *signal* × *model* points.

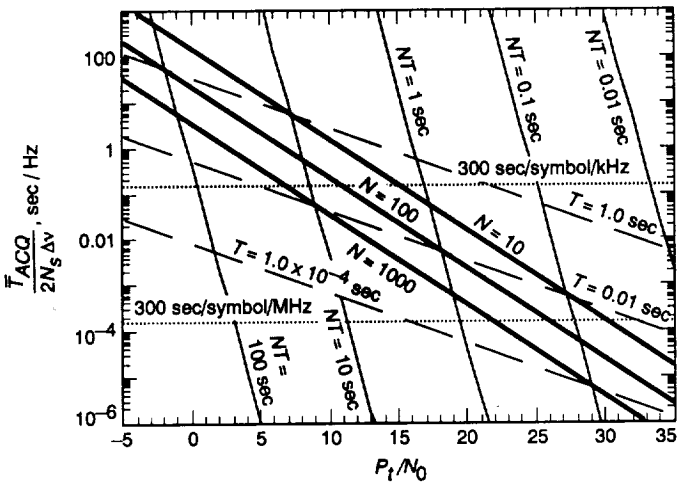

Fig. 9. Relationships between $T_{ACQ}/(2N_S\Delta\nu)$, N, T, and the P_t/N_0 required for ranging signal acquisition with P_{false} = 0.01 while P_{detect} = 0.99.

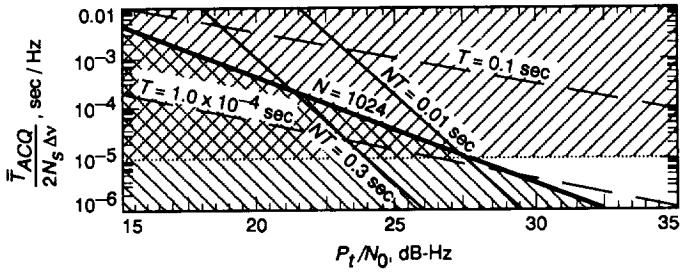

Fig. 10. Given the constraints $T_{ACQ}/(2N_S\Delta\nu) < 10^{-5}$ and N < 1024, the minimum P_t/N_0 enabling reliable ranging signal detection is 29 db–Hz.

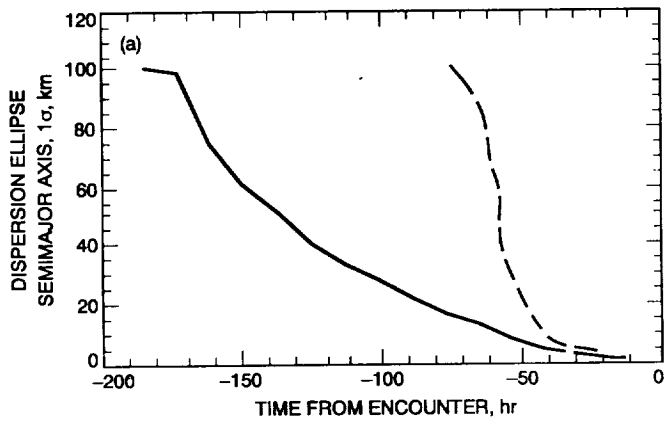

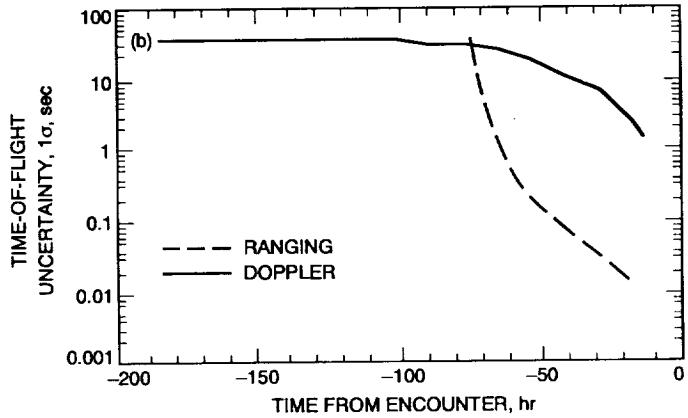

Fig. 11. Mars approach navigation dispersions (v_∞ = 3 km/sec): (a) aim-point uncertainty and (b) linearized time-of-flight uncertainty.

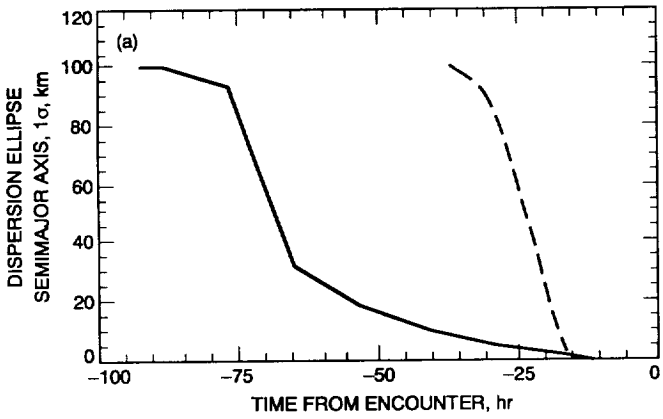

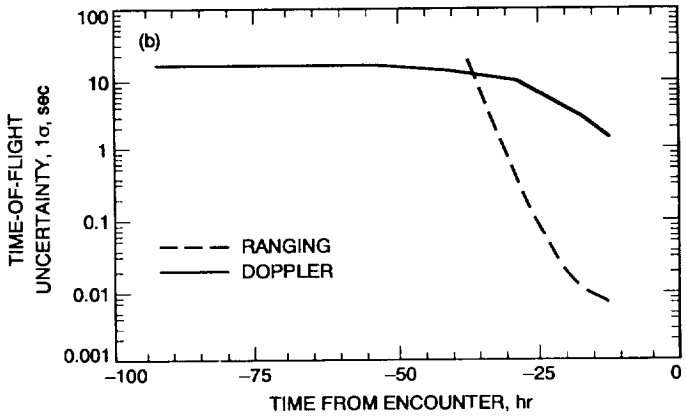

Fig. 12. Mars approach navigation dispersions (v_∞ = 6 km/sec): (a) aim-point uncertainty and (b) linearized time-of-flight uncertainty.

C-3

Appendix

Calculation of Relations between N and $(P_t/N_0)T$

As described in the article, the carrier detection strategy involves looking for Fourier resolution bins whose amplitude exceeds a threshold level. The detection threshold parameter, ξ, is selected such that the probability that the amplitude of the signal plus noise exceeds $\xi \times \{expected\ signal\ amplitude\}$ is 0.995. The probability of two consecutive signal detections when the signal is present, which shall be referred to as P_{detect}, is then 0.99. Calculation of the detection threshold must take into account signal amplitude losses resulting from two effects: (1) If the signal lies within the $1/T$ Hz range probed by the Fourier transform, it may differ from the model by up to $1/T$ Hz. Thus, each T-sec average of the $signal \times model$ phasor suffers amplitude loss because the phasor is not completely "stopped." (2) The signal will in general lie somewhere between Fourier resolution bins, so that the amplitude of the Fourier bin closest to the signal can be smaller than the true signal strength. The first effect can be ameliorated by discarding the Fourier resolution bins that lie toward the edges of the $1/T$ Hz frequency span, at the cost of increasing the number of Fourier transforms required to cover the entire search space of $\Delta\nu$ Hz. The fraction of Fourier resolution bins retained is referred to as χ. The second effect can be reduced by "oversampling," i.e., padding the data points with additional zeros, to decrease the frequency bin size of the Fourier transform. The degree of oversampling is described by a quantity, κ, which is equal to $N/(N + the\ number\ of\ padded\ zeros)$. Note that decreasing κ allows finer sampling of the Fourier transform at the cost of requiring increased computation (i.e., Fourier transforming a larger number of data points).

A reasonable selection of χ and κ, from the standpoint of minimizing acquisition time is $\chi = 1$ and $\kappa = 1/2$. For this choice of χ and κ, it can be shown that the detection threshold parameter, ξ, is given by the following formula:[1]

$$0.995 = 2 \int_{-1/2}^{1/2} du \int_{-1/4}^{1/4} dw (SNR_v)^2 e^{-0.5(\alpha SNR_v)^2} \times \int_{\xi}^{\infty} dr\ r\ e^{-0.5r^2 SNR_v^2} I_0(\alpha r SNR_v^2)$$

where $\alpha = (\sin(\pi u)/\pi u)(\sin(\pi w)/\pi w)$, I_0 is the 0th order modified Bessel function, and SNR_v is the voltage signal-to-noise ratio over NT sec, $\sqrt{2P_t/N_0 NT}$.

The probability that the noise amplitude in a given frequency bin exceeds ξSNR_v is $\exp(-0.5(\xi SNR_v)^2)$. Thus, the probability, P_{false}, that the noise amplitude exceeds ξSNR_v in at least one of N frequency bins is

$$P_{false} = 1 - (1 - \exp(-0.5(\xi SNR_v)^2))^N$$

The first equation allows numerical calculation of ξ as a function of SNR_v. Now if it is required that $P_{false} = 0.01$, then the second equation allows calculation of N as a function of SNR_v. But since $SNR_v = \sqrt{2P_t/N_0 NT}$, N may then be calculated as a function of $(P_t/N_0)T$. Over the range $6 < SNR_v < 12$, $(P_t/N_0)T \approx 29N^{-0.92}$.

In the case of detection of a PN-modulated carrier, the calculation is analogous, but SNR_v must be scaled by $(1 - 1/(2k_c))$, where $1/k_c$ chips is the model symbol offset step size. This factor accounts for the SNR_v loss during detection, due to the fact that the best alignment of the model and signal sequences may be off by as much as $1/2k_c$ chips. If the search is conducted in half-chip increments ($k_c = 2$) and $P_{detect} = 0.99$ while $P_{false} = 0.01$, then the relationship between $(P_t/N_0)T$ and N is $(P_t/N_0)T \approx 43N^{-0.91}$

[1] S. A. Stephens, "An Analysis of FFT Tone Acquisition," JPL Interoffice Memorandum 335.1-92-14 (internal document), Jet Propulsion Laboratory, Pasadena, California, May 14, 1992